Articles in PresS. Am J Physiol Heart Circ Physiol (August 5, 2016). doi:10.1152/ajpheart.00197.2016

Adaptation of the Cerebrocortical Circulation to Carotid Artery Occlusion Involves Blood Flow Redistribution between Cortical Regions and is Independent of eNOS

Andreas **Polycarpou**[1], László **Hricisák**[1], András **Iring**[1,2], Daniel **Safar**[1], Éva **Ruisanchez**[1], Béla **Horváth**[1], Péter **Sándor**[1], Zoltán **Benyó**[1]

[1]Institute of Clinical Experimental Research, Semmelweis University, Budapest, Hungary

[2]Max Planck Institute for Heart and Lung Research, Department of Pharmacology, Bad Nauheim, Germany

Authors' contributions: ZB, PS and BH planned and supervised the project; BH and AI introduced laser-speckle imaging for studying cerebrocortical microcirculation in mice and optimized the experimental procedures in preliminary experiments; AP, LH, AI and DS performed the experiments; AP, LH, DS and ÉR evaluated the experiments and analyzed the data; AP and ÉR prepared the figures and tables; AP, LH, PS and ZB wrote the manuscript.

Correspondence and request for reprints: Zoltán Benyó, MD, PhD, DSc
Institute of Clinical Experimental Research, Semmelweis University
Address: Tűzoltó u. 37-47., H-1094 Budapest, Hungary
Postal Address: POB 2, H-1428 Budapest, Hungary
Tel.: +36-1-210-0306, Fax: +36-1-334-3162
E-mail: benyo.zoltan@med.semmelweis-univ.hu

Running head: Adaptation of the cerebrocortical microcirculation to CAO

Abstract

Cerebral circulation is secured by feed-forward and feed-back control pathways to maintain and eventually reestablish the optimal oxygen and nutrient supply of neurons in case of disturbances of the cardiovascular system. Using the high temporal and spatial resolution of laser-speckle imaging we aimed to analyze the pattern of cerebrocortical blood flow (CoBF) changes after unilateral (left) carotid artery occlusion (CAO) in anesthetized mice in order to evaluate the contribution of macrovascular (circle of Willis) vs. pial collateral vessels as well as that of endothelial nitric oxide synthase (eNOS) to the cerebrovascular adaptation to CAO. In wild-type mice CoBF reduction in the left temporal cortex started immediately after CAO, reaching its maximum (-26%) at 5-10 s. Thereafter, CoBF recovered close to the pre-occlusion level within 30 s indicating the activation of feed-back pathway(s). Interestingly, the frontoparietal cerebrocortical regions also showed CoBF reduction in the left (-17-19%) but not in the right hemisphere, although these brain areas receive their blood supply from the common azygos anterior cerebral artery in mice. In eNOS-deficient animals the acute CoBF reduction after CAO was unaltered, and the recovery was even accelerated as compared to controls. These results indicate that (i) the Willis circle alone is not sufficient to provide an immediate compensation for the loss of one carotid artery, (ii) pial collaterals attenuate the ischemia of the temporal cortex ipsilateral to CAO at the expense of the blood supply of the frontoparietal region, and (iii) eNOS, surprisingly, does not play an important role in this CoBF redistribution.

New & Noteworthy

Temporal and spatial pattern of cerebrocortical blood flow changes after unilateral carotid artery occlusion has been determined by laser-speckle imaging in mice. The main conclusions are that microvascular feed-back mechanisms involving pial collaterals aid the Willis circle in the cerebrovascular adaptation, and eNOS, surprisingly, is not important in this process.

Keywords: cerebrocortical microcirculation, carotid artery occlusion, cerebrovascular regulation, pial collateral circulation, eNOS

Introduction

An important characteristic of cerebral circulation is the remarkable steadiness of the cerebral blood supply at rest as well as during disturbances of the systemic circulation. In order to meet the high metabolic demands of neurons, astrocytes and pericytes (approx. 7 mg glucose / 100 g grey matter / min), the brain must be supplied continuously by approximately 50 ml / 100g / min arterial blood, carrying 3.5 ml / 100 g / min oxygen on average (45). Under physiological conditions, despite fluctuations of the systemic mean arterial blood pressure (MABP) between 60-140 mmHg, changes in the partial pressure of arterial blood gases, and alterations of global or regional neuronal metabolic activity, the necessary rate of cerebral blood flow is ensured by metabolic, myogenic, endothelial and neural regulatory mechanisms (4).

The effectiveness of these control systems, however, is not unlimited. Cerebral ischemia is among the most common causes of death: it contributes to 87% of all strokes (36), and approximately 30% of strokes are caused by occlusive diseases of the carotid arteries (20). The overwhelming majority involve the occlusion of the internal carotid arteries (ICA), but the occlusion of the common carotid artery (CCA) is also responsible for approximately 0.24-5.0% of stroke cases (1). The pathological mechanisms that can lead to either gradual or sudden carotid artery occlusion include atherosclerosis, thrombosis superimposed on the atherosclerotic plaque, and carotid artery dissection. Among these, atherosclerosis (by far the most common occlusive disease affecting the carotid arteries) may lead to either symptomatic or asymptomatic carotid artery stenosis. The annual stroke rate was found to be 13% in case of high-grade stenosis (luminal occlusion over 70%), and 7% in moderate stenosis (luminal occlusion between 30-69%) (49).

It is surprising that following verified partial or complete carotid artery stenosis no serious neurological deficits can be demonstrated in the majority of patients (19). After ligation of the CCA (a method historically used for treating ICA aneurysms), focal neurological deficits were noted only in a minority of the cases and immediate neurological complications developed only in 4.2-6.4% of the patients (31, 37). These important observations indicate that in spite of the closure of one critically important source of the arterial blood supply to the brain (CCA), yet unknown but very efficient compensatory mechanisms step in to maintain sufficient blood flow to the neurons and keep them alive without significant clinical signs.

Theoretically, there are at least three possible compensatory mechanisms which may be involved in the cerebrovascular adaptation to carotid artery occlusion (CAO). *First,* compensation may occur in large intracranial vessels within the circle of Willis, where CAO induces pressure, flow and resistance changes. This theory is supported by the observations that in most patients ligation of the CCA results not only in a reduced flow, but also in an immediate reversal of blood flow in the ICA (i.e. away from the brain) for 1-18 hours, after which the flow returns to the normal forward direction with a reduced rate of 24-50% as compared to its pre-occlusion level (55). Interestingly, transgenic mice lacking the anterior connection between the two sides of the circle of Willis were reported to develop severe neurological symptoms and died after unilateral ligation of the CCA indicating the major importance of the intracranial collaterals in the cerebrovascular adaptation to CAO (39).

The *second* possibility for cerebrovascular adaptation to CAO is based on the theory that under physiological conditions there is a balance between the extracranial collateral circulation of the head and neck area and the intracranial collateral circulation (Willis circle) via occipital, facial and maxillary branches of the external carotid artery (ECA). This balance and, consequently, the blood flow in the ICA and in the ECA can change significantly under pathological conditions. The anatomy of the Willis circle varies greatly (27), and in case of an anatomically inadequate circle of Willis, reversal of the flow in the ECA following CCA occlusion may serve as an immediate collateral blood supply for the ICA (55).

A *third* possible mechanism could be the recruitment of pial collateral vessels that form anastomoses between the terminal cortical branches of the major cerebral arteries (i.e. the anterior, middle, and posterior cerebral arteries) throughout the surface of the brain. The aim of the present study was to investigate the potential role of these small pial collateral arteries in the cerebrovascular adaptation to CCA occlusion, with special emphasis on the role of endothelial nitric oxide synthase (eNOS), a constitutively expressed enzyme, producing nitric oxide (NO) in the cerebral circulation. NO is known to play a major role in flow-induced vasodilation of cerebral vessels, in metabolic control of the cerebral blood flow and in neurovascular coupling (12, 13, 51). Therefore, the participation and potential role of eNOS and its product, NO, in cerebrovascular autoregulation following complete occlusion of the left CCA was also investigated. Laser speckle imaging was used to determine and to compare regional cerebrocortical blood flow (CoBF) changes following permanent unilateral CCA occlusion in control wild type (WT) and eNOS-deficient (eNOS-KO) mice.

Methods

The experiments were performed on WT (n=12) and eNOS-KO (n=11) adult male C57Bl6 mice (body weight 25-35 g) according to the guidelines of the Hungarian Law of Animal Protection (28/1998). All procedures were approved by the National Scientific Ethical Committee on Animal Experimentation (PEI/001/2706-13/2014). The mice were anesthetized with 2% inhaled isoflurane during femoral artery catheterization, and with intraperitoneally (i.p.) applied ketamine (100 μg / g bw. Calypsol, Richter Gedeon Plc., Budapest, Hungary) and xylazine (10 μg / g bw. CP-Xylazine, CP-Pharma GmbH, Burgdorf, Germany) throughout the rest of the experiment. The depth of the anesthesia was frequently tested during the experiments by checking the plantar nociception or corneal reflex, and additional anesthetic was administered as necessary. The left femoral artery was cannulated under a stereomicroscope, and it was used for continuous systemic arterial pressure measurement, and, at the end of each experiment, the same cannula was used for arterial blood sampling for determination of blood gas tensions and acid/base parameters. Body temperature was maintained between 36 and 37 °C throughout the experiment by using a heating pad, controlled by a rectal probe.

Following femoral artery cannulation and intraperitoneal ketamine/xylazine administration, the trachea was exposed and the mice were allowed to breathe spontaneously through an intratracheal cannula. Subsequently, the carotid sheath was gently dissected under microscopic magnification (with particular care to preserve the intact vagus nerve) and a ligature with a loose knot was placed around the left CCA.

For the measurement of the CoBF, the head of the mouse was secured in a stereotaxic head holder, and the skull was exposed by retracting the scalp following a midline incision. The CoBF was measured by using the laser-speckle imaging method (PeriCam PSI, Perimed AB, Järfälla, Stockholm, Sweden) in three carefully determined and standardized cortical regions of interest (ROI): frontal, parietal, and temporal cortices of both hemispheres. The reason for choosing these specific cerebral regions for CoBF determinations was that each of these regions is supplied by different cerebral arteries (43). In this way one may more accurately and reliably assess the CoBF alterations and redistributions throughout the entire surface of the cerebral hemispheres following unilateral CAO. The ROIs for the CoBF measurements and the blood supply to these regions are depicted in Figure 1.

Two key factors were taken into consideration in order to select the required ROIs as accurately as possible: 1) any visible major cerebral arteries, veins and venous sinuses were excluded from the selected ROIs, 2) the cerebrocortical area that is known to have the highest density of microvascular anastomoses between the main cerebral arteries was also excluded from the ROI selection as this area has dual blood supply (28, 29, 50). The localization of the pial anastomoses between the territories of the middle and anterior cerebral arteries (MCA and ACA) has been determined by Maeda et al (28, 29). According to these coordinates we aimed to set the temporal region laterally, whereas the frontal and parietal regions medially from the zone of anastomoses in order to clearly demarcate the territories supplied by the MCA and the ACA (Figure 1). (It has to be noted that in mice the two ACA fuse and give rise to the azygos anterior cerebral artery (AACA) which supplies the frontoparietal cerebral cortex of both hemispheres (43).) The CoBF of the frontal and parietal regions have been evaluated separately because the parietal region may receive additional pial collaterals from the posterior cerebral artery (5), which might improve the capacity of microcirculatory adaptation in this region.

Prior to starting the CoBF measurements, atipamezole (Sigma-Aldrich Co., St. Louis, MO, USA; 1 μg/g i.p.) was administered as an antidote to xylazine, to reverse xylazine's alpha-2 agonistic effects, and in this way to ensure a stable blood pressure throughout the experiment. Five to ten minutes were allowed for atipamezole's effect to get established. Following this, 5 to 10 minutes were allowed to acquire baseline data of CoBF and blood pressure. Arterial blood pressure was measured and recorded continuously during the entire time of the experiment.

After acquiring the baseline data, the left CCA was occluded by tightening the loose knot around this vessel. The CoBF parameters, measured by the laser-speckle technique were as follows: (i) average steady state CoBF value for one minute preceding CAO that was used as a 100% reference CBF baseline value, (ii) the initial drop of the CBF upon CAO, and (iii) the dynamics of the CBF changes ("recovery") following the initial drop of CBF, for 5 minutes after the CAO. Before terminating an experiment, arterial blood was sampled via the femoral artery cannula to determine arterial blood gas tensions and acid/base parameters. If arterial O_2 saturation was less than 90 % or CO_2 tension was out of the range of 25-55 mmHg the experiment was excluded from the evaluation. Complete occlusion of the CCA has been verified in each animal by inspection under a stereomicroscope.

Values in the text, figures and tables are presented as mean ± SEM; *n* represents the number of mice tested. Statistical analysis for the arterial blood gas and acid/base parameters was performed using Student's unpaired *t*-test, whereas for the MABP and CoBF two-way ANOVA with Bonferroni's post hoc test was used. A *P* value of less than 0.05 was considered to be statistically significant.

Results

Systemic physiological parameters

Baseline mean arterial blood pressure (MABP) was stable and within the autoregulatory range of the cerebral circulation both in WT and in eNOS-KO animals (Figure 2A.). However, in accordance with reported observations (46, 47), the MABP of eNOS-KO mice was approximately 25 mmHg higher and more variable as compared to controls. CAO induced only minor MABP changes in both experimental groups, although the elevation of the MABP was more pronounced and sustained in mice deficient in eNOS (Figure 2B.). Importantly, arterial blood gas and acid-base parameters were within the physiological range, and were not different between WT and eNOS-KO animals (Table 1.).

Effects of CAO on the regional CoBF in WT mice

The first aim of the present study was to analyze the temporal pattern of CAO-induced CoBF changes in the different cerebrocortical regions in order to answer two questions: (i) does the adaptation of cerebral circulation to the altered hemodynamic state after CAO involve active vasodilation, and if so, (ii) do pial collaterals between territories of the main cerebrocortical arteries (AACA and MCA) contribute to this process? We assumed that analysis of the temporal pattern of CoBF changes can be used to answer the first question, whereas development of regional differences within the cerebral cortex can indicate CoBF redistribution via pial anastomic vessels.

In WT mice CoBF declined rapidly in all three ipsilateral cerebrocortical regions after CAO (Figures 3, 4A, 4C and 4E). The CoBF reduction was obvious in the temporal cortex within 1 s and reached the maximal level at 5-10 s (Figures 3 and 4E). The CoBF of the frontal and

parietal regions ipsilateral to CAO decreased simultaneously with that of the temporal cortex (Figures 4A, 4C and 4E), although their CoBF reduction was significantly less pronounced (Figure 5A). At approximately 10 s after CAO the CoBF started to increase in all cortical regions, and returned close to the baseline level within 30 s (Figures 3, 4A, 4C and 4E). Interestingly, in the subacute phase (i.e. 1-5 min after CAO) the CoBF reduction was less than 10% in all three cortical regions without any significant inter-regional difference (Figure 5B). One can conclude from these observations that the existing macrovascular connections (i.e. the circle of Willis) are not sufficient to immediately and completely compensate for the loss of one carotid artery, and active vasodilation is required to accommodate cerebrocortical circulation to the altered hemodynamic situation. In addition, the observation that CAO resulted in a significant CoBF reduction of the frontoparietal region as compared to the contralateral hemisphere in spite of the common blood supply of these brain areas by the AACA indicates redistribution of the CoBF via pial collaterals to the severely ischemic temporal cortex on the side of CAO.

Effects of CAO on the regional CoBF in eNOS-KO mice

Our observations in WT mice indicated that the adaptation of cerebrocortical circulation to unilateral CAO involves pial and/or microvascular vasodilation. Since endothelial NO is a major regulator of the microvascular resistance in cerebral circulation (12, 13) we tested the hypothesis that eNOS may play a significant role in the adaptation to CAO. Changes of the regional CoBF after CAO in eNOS-KO animals, however, resembled in many ways the findings in WT mice (Figure 4B, 4D, 4F). The temporal pattern showed an acute drop followed by gradual recovery in all three cerebrocortical regions under investigation. In addition, similarly to WT animals, the acute reduction was most pronounced in the temporal cortex (Figure 5A), whereas during the subacute phase this inter-regional difference disappeared (Figure 5B). Surprisingly, the percentual changes of the regional CoBF showed no significant difference between eNOS-KO and WT mice either during the acute (Figure 5A) or the subacute (Figure 5B) phase after CAO. In fact, the recovery even appeared to be more rapid in the temporal cortex of eNOS KO mice as compared to WT controls (Figures 4E and 4F).

Discussion

The present study was designed to investigate the cerebrovascular compensatory mechanisms developing after unilateral occlusion of the CCA. We aimed to answer three basic questions: Does the adaptation of cerebral circulation to the altered hemodynamic state after CAO involve flow changes and active vasodilation in the *large arteries* of the Willis circle? Do *small pial collateral arteries* between territories of the main cerebrocortical arteries (AACA and MCA) contribute to the redistribution of the CoBF? Is *eNOS* involved in the cerebrovascular adaptation to CAO?

In our experiments CoBF was reduced rapidly and simultaneously in the ipsilateral frontal, parietal and temporal cerebrocortical regions after CAO (Figure 4.). However, after the acute phase, CoBF started to increase in the affected regions and returned close to the baseline level within 30 s, and 1-5 min after CAO the reduction of CoBF was less than 10% in all three cortical regions without any significant inter-regional differences. Similar dynamics of initial CoBF changes have been reported in the parietal cortex of anesthetized rats (35), followed by an overshoot of the blood flow, which was absent in our present study. One can conclude from these observations that the existing macrovascular connections (i.e. the arteries of the Willis circle) are not sufficient to compensate immediately and completely for the loss of one CCA, and that active cerebral vasodilation is required to adapt cerebrocortical circulation to the altered hemodynamic situation.

In our present study unilateral closure of the CCA resulted in instant, significant CoBF reduction in the temporal cortex of the ipsilateral hemisphere. This was expected, since this region is supplied by the MCA originating from the circle of Willis close to the influx of the internal carotid artery. However, it was unexpected that the ipsilateral frontal and parietal cortices also showed reduced blood perfusion as compared to the contralateral ones, although in mice all of these brain regions receive their blood supply from the same artery, namely the AACA. This observation can only be explained by a draining effect through connections between the territories of the MCA and AACA, via pial anastomoses. The presence of such connections (16, 28, 29, 52), as well as their importance after MCA occlusion (50, 56) have already been demonstrated. However, to the best of our knowledge, the present study is the first indication for the involvement of small pial anastomoses in the acute adaptation of cerebrocortical circulation to CCA occlusion. We assume that a steal phenomenon may develop, and the blood flow of pial arteries supplying the fronto-parietal regions is drained

via pial anastomic vessels to the more ischemic temporal cortex of the hemisphere ipsilateral to the CCA occlusion. Interestingly, 15 days after CAO, markedly enlarged pial anastomic connections have been reported in mice indicating the significant contribution of these collateral vessels also to the chronic adaptation of the cerebrocortical circulation to CAO (16) and similar results have been obtained 6 days after MCA occlusion in mice (56).

It is an important question whether the simple existence of collaterals is sufficient for the normalization of cerebrocortical circulation after CAO, or their active dilation is also required for the compensation. To answer this question, the distribution of cerebrovascular resistance along the arterial vessel tree has to be considered. Table 2 gives an overview of the experimental data available. It can be concluded that large cerebral vessels, including the circle of Willis, significantly contribute to the total cerebrovascular resistance, since in normotensive animals the blood pressure in the first order branches of the MCA is 39-54% lower than the systemic mean arterial pressure. The contribution of pial vessels, however, is also significant, evidenced by the additional 10-32% pressure drop from the first order MCA branches to the penetrating arteries/arterioles. These data indicate that vasodilation both in the circle of Willis and pial arteries could improve the blood perfusion of the MCA territory after CAO. The observations that during changes in systemic blood pressure small pial vessels as well as large cerebral arteries simultaneously contribute to the CoBF autoregulation by changing their diameter/resistance (17, 18, 44) suggest that adaptation of the cerebrocortical circulation to CAO may also involve an active vasodilation both in the small and the large cerebral arteries. The temporal pattern of the recovery of CoBF after CAO in our present study also indicates that vasodilation has to develop in order to achieve the optimal level of adaptive responses in the cerebrovascular system.

An additional mechanism, which can aid the normalization of the brain's regional blood perfusion after CAO, is the reduction of the resistance in intraparenchymal microvessels. These changes can be governed by different regulatory pathways, including myogenic, metabolic, neurogenic and endothelial mechanisms. Reduction of the myogenic tone as a response to the smaller transmural pressure, (i.e. weaker wall tension due to the reduced intraluminar pressure), enhanced release of vasodilatory neurotransmitters from the neurons and nerve endings and accumulation of metabolic end-products as a result of insufficient tissue blood perfusion are certainly among the regulatory factors. Several lines of evidence, however, indicate that vasoactive substances - especially NO - released from the

307 microvascular endothelium in response to the reduction of cerebral blood supply are crucially
308 important contributors to the maintenance of cerebral blood flow.

309 NO has been shown to play a major, complex role in the regulation of cerebral circulation. A
310 multitude of in vitro as well as in vivo studies support that it contributes significantly to the
311 control of the resting cerebral vascular tone, it has a potent cerebral vasodilatory effect by
312 mediating endothelium-dependent vascular relaxation, it acts directly on vascular smooth
313 muscle, and plays a significant role in the mediation of CO_2-induced as well as hypoxia-
314 induced cerebral vasodilation. It is well documented that following its release by the
315 endothelium, NO diffuses into the vascular smooth muscle cells, where, by activating soluble
316 guanylyl cyclase (sGC), it increases the intracellular concentration of cyclic guanine
317 monophosphate (cGMP), which in turn eventually leads to smooth muscle relaxation and
318 vasodilation (40). There is also evidence to suggest that NO causes vasodilation not only
319 through cGMP-mediated mechanisms, but in certain species also by activating potassium
320 channels (for review see (13)).

321 *In vitro studies,* using large cerebral arteries provided most of the experimental evidence
322 regarding endothelium-mediated cerebral vasodilation. It was proved that NO exerts a resting
323 tonic vasodilatory effect on cerebral circulation, since the basal cGMP level was found to be
324 significantly greater in cerebral arteries having intact endothelium, as compared to those from
325 which the endothelium was removed (8, 24, 48). Cerebral vasodilation in response to
326 acetylcholine and to other receptor-mediated agonists (such as serotonin, substance P and
327 ADP), which activate eNOS by increasing intracellular calcium levels, was shown to be NO-
328 dependent (for review see (12)).

329 *In vivo studies* (10) showed that topical application of the NOS inhibitor L-NMMA leads to
330 constriction of the rat basilar artery, an effect that was reversed upon administration of the
331 NO-precursor molecule L-arginine. In several species, under basal conditions, local and
332 systemic application of NOS inhibitors was shown to provoke cerebral vasoconstriction and a
333 decrease in CoBF (12). Due to the fact that systemic NOS inhibitors lead to an increase in the
334 cerebral and the peripheral vascular resistance, it is logical to infer that resting levels of NO
335 are necessary to maintain the resistance vessels in a relaxed state (22). In other studies, which
336 tested mice and piglet pial arterioles, L-arginine administration was shown to dilate pial
337 arterioles in a dose-dependent manner (7, 41).

NO was also shown to possess a basal inhibitory effect, which buffers spontaneous cerebral vasomotion (9), inhibits vasoconstriction in response to substances such as norepinephrine and serotonin (for review (12)), and thereby contributes to the maintenance of a stable CoBF. Studies have demonstrated that administration of non-selective NOS inhibitors leads to an enhancement of cerebral vascular oscillations (2, 9, 15, 21, 26), whereas NO caused an attenuation of vasomotion (22).

Involvement of NO in the regulation of cerebral circulation during ischemia has also been extensively studied. An acute increase in NO concentration within minutes following ischemia has been observed (30), which, due to its rapidity, was attributed to an ischemia-induced activation of the constitutive eNOS enzyme (57). Similar observations have also been made in a study, which utilized MCA occlusion to induce cerebral ischemia (23). The potentially beneficial consequence of an increase in NO during ischemia is the maintenance of CoBF through vasodilation and the inhibition of platelet and leukocyte aggregation (13). These effects, therefore, serve to limit the infarct's size and reduce brain damage. The potential protective effect of endothelium-derived NO during and after cerebral ischemia has been pointed out by studies, which utilized eNOS-deficient mice (13). Administration of L-arginine after MCA occlusion leads to the dilation of pial arterioles, to a reduction of infarct size and to an increase of CoBF (33, 34). On the other hand, NOS inhibitors were reported to induce either no effect or an increase in the ischemia-induced cerebral infarct size (for review see (12)).

Based on the aforementioned literary data we hypothesized that endothelium-derived NO may play an important role in the cerebrovascular adaptation to CAO. According to our results, however, the CAO-induced acute ipsilateral CoBF reduction in the three investigated cerebrocortical regions of the eNOS-KO animals was not different from that of the control, wild-type mice, neither in the acute, nor in the subacute phase of the CAO. These results indicate that eNOS does not appear to play an important role in the CoBF redistribution after CAO. In fact, the faster recovery of CoBF in the temporal cortex of eNOS-KO compared to WT mice can be attributed to the elevated MABP in these animals. It has been previously described that systematically administered NOS inhibitors can increase arterial pressure in a dose-dependent manner and therefore enhance blood flow in collateral vessels, which supply cerebral regions that were rendered ischemic though arterial occlusion (32).

Limitations of our experimental approach have also to be considered during the interpretation of our findings. The fact, that eNOS-KO mice showed unaltered cerebrocortical adaptation following CAO-induced reduction of CoBF does not necessarily exclude the role of NO in these mechanisms. Several lines of evidence indicate that endothelium-dependent and -independent vasodilator pathways may get activated in order to compensate for the absence of endothelial NO production and therefore the phenotypic consequences of the eNOS gene deletion may underestimate the importance of eNOS under physiological conditions. For instance, neuronal NOS (nNOS) may be upregulated in the absence of eNOS. It has been reported that eNOS- and nNOS-derived NO is simultaneously involved in a variety of cerebrovascular functions, including the regulation of resting cerebral blood flow (3), CO_2-mediated (38, 53) and neuronally induced vasodilation (6, 14) as well as flow-metabolism coupling (11, 13). Interestingly, it has been shown that nNOS within the brain is not only found in neurons, glial cells and perivascular nerves (12), but also in the endothelium of the cerebral vasculature (3).

In conclusion, in the present study, taking advantage of the high temporal and spatial resolution of laser-speckle imaging, attempts were made to gain insight into the mechanisms of the adaptation of cerebrocortical microcirculation to unilateral occlusion of the common carotid artery. The transient reduction of the CoBF in all investigated regions of the ipsilateral hemisphere clearly indicate that, in spite of the well-developed macro- and microvascular collateral network and the robust myogenic control of the vascular tone, the feed-forward mechanisms of cerebrovascular regulation are not sufficient to prevent cerebral ischemia after CAO. The temporal pattern of the CoBF recovery after CAO suggests the significance of an active cerebrovascular vasodilator mechanism driven by metabolic, endothelial or neuronal signals. Surprisingly, eNOS-dependent vasodilation does not appear to be involved in this process. In contrast, intracortical redistribution of the CoBF, presumably via pial anastomoses between the MCA and AACA, appears to attenuate the ischemia of the most severely affected temporal cortex at the expense of reducing the blood perfusion of the frontoparietal regions.

Acknowledgements

The authors wish to acknowledge the seminal findings and methodological achievements of Prof. Minoru Tomita, MD, PhD (1934–2010) regarding the physiological and pathophysiological functions of pial collateral vessels. The authors are grateful to Dr. Erzsébet Fejes for critically reading the manuscript as well as to Dr. Péter Dancs and András Kucsa for graphic artwork. This study has been supported by the Hungarian Scientific Research Fund (OTKA K-62375, K-101775 and K-112964).

Figure Legends

Fig. 1.

Localization of cerebrocortical regions on a representative laser-speckle image (panel A) and schematic illustration of their supplying vessels (panel B). Small arrows indicate pial anastomoses between the territories supplied by the middle cerebral arteries (MCA) and the azygos anterior cerebral artery (AACA). ICA, internal carotid artery; ACA, anterior cerebral artery; PCA, posterior cerebral artery; FP, frontal pole; B, bregma; λ, lambda

Fig. 2.

Mean arterial blood pressure (MABP) in WT (n=12) and eNOS-KO (n=11) mice (panel A) and its changes after left carotid artery occlusion (CAO) (panel B). CAO was performed at time point „0 s". MABP was significantly higher in eNOS-KO animals at all time points, whereas ΔMABP differed from 210 s (*P<0.05, **P<0.01, ***P<0.001 between WT and eNOS-KO with 2-way ANOVA and Bonferroni's post hoc test). Note the enhanced time resolution between (panel A) or before (panel B) the dashed lines.

Fig. 3.

Regional changes of the cerebrocortical blood flow (CoBF) at different time points after left carotid artery occlusion (CAO), shown as differerence images compared to the baseline CoBF, i.e. the averaged CoBF in 1 min preceding CAO. CAO was performed at time point „0". AU, arbitrary units; F, P and T indicate the frontal, parietal and temporal regions, respectively according to the coordinates described on Fig. 1A.

Fig. 4.

Regional cerebrocortical blood flow (CoBF) in WT (n=12, panels A, C and E) and eNOS-KO (n=11, panels B, D and F) before and after carotid artery occlusion (CAO). CoBF is expressed as percentage of the baseline, i.e. the averaged values in 1 min preceding CAO. Blue and red symbols represent CoBF in the ipsilateral and contralateral hemispheres, respectively. (*P<0.05, **P<0.01, ***P<0.001 vs. „Contralateral" with 2-way ANOVA and Bonferroni's post hoc test). Note the enhanced time resolution between the dashed lines.

Fig. 5.

Acute (panel A) and subacute (panel B) reductions of the regional cerebrocortical blood flow (CoBF) in the ipsilateral hemisphere of WT (filled bars, n=12) and eNOS-KO (open bars, n=11) mice after left carotid artery occlusion (CAO). CoBF values have been determined at their minimum („Acute") or at 5 min after CAO („Subacute"), and reductions were expressed as percentage of the baseline, i.e. the average CoBF in 1 min preceding CAO. (*$P<0.05$, **$P<0.01$ vs. „Frontal"; $^{\#}P<0.05$, $^{\#\#}P<0.01$ vs. „Parietal" with 2-way ANOVA and Bonferroni's post hoc test.)

Tables

Table 1. Arterial blood gas and acid-base parameters in the experimental groups

Variable	WT (n=12)	eNOS-KO (n=11)
PaO_2 (mmHg)	113.5 ± 5.1	112.6 ± 5.1
O_2-Saturation (%)	97.5 ± 0.4	97.7 ± 0.3
$PaCO_2$ (mmHg)	41.2 ± 2.1	37.6 ± 2.5
pH	7.30 ± 0.02	7.32 ± 0.02
SBE (mmol/l)	-6.0 ± 1.0	-6.4 ± 0.7
$[HCO_3^-]$ (mmol/l)	19.7 ± 0.9	18.7 ± 0.6
Hematocrit (%)	38.4 ± 1.0	39.4 ± 1.2

Table 2. Blood pressure levels in different segments of the MCA expressed as percentage of the systemic MABP

Species	Anesthesia	Systemic MABP (mmHg)	Blood Pressure (% of MABP) in Order Branch of the MCA				Reference
			1st	2nd	3rd	4th*	
Rat	Inactin	122	46%	43%	22%		*Harper et al. (17, 18)*
Cat	Pentobarbital	70-140	61%	57%	55%	51%	*Shapiro et al. (44)*
Cat	Pentobarbital	120		74%**		42%**	*Kontos et al. (25)*
Cat	Ketamine + Halothane + N_2O	87			47%		*Schmidt-Kastner et al. (42)*
Cat	Chloralose + Urothane + Pancuronium	115-117				60-63%	*Yamaguchi et al. (54)*

The level of pressure drop indicates the segmental distribution of cerebrovascular resistance.

*Penetrating arterioles

**Recalculated from resistance values

REFERENCES

1. **Bajko Z, Balasa R, Motataianu A, Maier S, Chebut OC, and Szatmari S**. Common carotid artery occlusion: a case series. *ISRN Neurol* 2013: 198595, 2013.

2. **Behzadi Y, and Liu TT**. An arteriolar compliance model of the cerebral blood flow response to neural stimulus. *Neuroimage* 25: 1100-1111, 2005.

3. **Benyo Z, Lacza Z, Hortobagyi T, Gorlach C, and Wahl M**. Functional importance of neuronal nitric oxide synthase in the endothelium of rat basilar arteries. *Brain Res* 877: 79-84, 2000.

4. **Benyo Z, Ruisanchez E, Leszl-Ishiguro M, Sandor P, and Pacher P**. Endocannabinoids in cerebrovascular regulation. *Am J Physiol Heart Circ Physiol* 310: H785-801, 2016.

5. **Brozici M, van der Zwan A, and Hillen B**. Anatomy and functionality of leptomeningeal anastomoses: a review. *Stroke* 34: 2750-2762, 2003.

6. **Busija DW, Bari F, Domoki F, and Louis T**. Mechanisms involved in the cerebrovascular dilator effects of N-methyl-d-aspartate in cerebral cortex. *Brain Res Rev* 56: 89-100, 2007.

7. **Busija DW, Leffler CW, and Wagerle LC**. Mono-L-arginine-containing compounds dilate piglet pial arterioles via an endothelium-derived relaxing factor-like substance. *Circ Res* 67: 1374-1380, 1990.

8. **Cosentino F, Sill JC, and Katusic ZS**. Endothelial L-arginine pathway and relaxations to vasopressin in canine basilar artery. *Am J Physiol* 264: H413-418, 1993.

9. **Dirnagl U, Lindauer U, and Villringer A**. Nitric oxide synthase blockade enhances vasomotion in the cerebral microcirculation of anesthetized rats. *Microvasc Res* 45: 318-323, 1993.

10. **Faraci FM**. Role of nitric oxide in regulation of basilar artery tone in vivo. *Am J Physiol* 259: H1216-1221, 1990.

11. **Faraci FM, and Brian JE, Jr.** 7-Nitroindazole inhibits brain nitric oxide synthase and cerebral vasodilatation in response to N-methyl-D-aspartate. *Stroke* 26: 2172-2175; discussion 2176, 1995.

12. **Faraci FM, and Brian JE, Jr.** Nitric oxide and the cerebral circulation. *Stroke* 25: 692-703, 1994.

13. **Faraci FM, and Heistad DD**. Regulation of the cerebral circulation: role of endothelium and potassium channels. *Physiol Rev* 78: 53-97, 1998.

14. **Gotoh J, Kuang TY, Nakao Y, Cohen DM, Melzer P, Itoh Y, Pak H, Pettigrew K, and Sokoloff L**. Regional differences in mechanisms of cerebral circulatory response to neuronal activation. *Am J Physiol Heart Circ Physiol* 280: H821-829, 2001.

15. **Griffith OW, and Kilbourn RG**. Nitric oxide synthase inhibitors: amino acids. *Methods Enzymol* 268: 375-392, 1996.

16. **Guo H, Itoh Y, Toriumi H, Yamada S, Tomita Y, Hoshino H, and Suzuki N**. Capillary remodeling and collateral growth without angiogenesis after unilateral common carotid artery occlusion in mice. *Microcirculation* 18: 221-227, 2011.

17. **Harper SL, and Bohlen HG**. Microvascular adaptation in the cerebral cortex of adult spontaneously hypertensive rats. *Hypertension* 6: 408-419, 1984.

18. **Harper SL, Bohlen HG, and Rubin MJ**. Arterial and microvascular contributions to cerebral cortical autoregulation in rats. *Am J Physiol* 246: H17-24, 1984.

19. **Hennerici M, Aulich A, Sandmann W, and Freund HJ**. Incidence of asymptomatic extracranial arterial disease. *Stroke* 12: 750-758, 1981.

20. **Henry M, Polydorou A, Klonaris C, Henry I, Polydorou AD, and Hugel M**. Carotid angioplasty and stenting under protection. State of the art. *Minerva Cardioangiol* 55: 19-56, 2007.

21. **Horvath B, Lenzser G, Benyo B, Nemeth T, Benko R, Iring A, Herman P, Komjati K, Lacza Z, Sandor P, and Benyo Z**. Hypersensitivity to thromboxane receptor mediated cerebral vasomotion and CBF oscillations during acute NO-deficiency in rats. *PLoS One* 5: e14477, 2010.

22. **Iadecola C, Pelligrino DA, Moskowitz MA, and Lassen NA**. Nitric oxide synthase inhibition and cerebrovascular regulation. *J Cereb Blood Flow Metab* 14: 175-192, 1994.

23. **Kader A, Frazzini VI, Solomon RA, and Trifiletti RR**. Nitric oxide production during focal cerebral ischemia in rats. *Stroke* 24: 1709-1716, 1993.

24. **Kim P, Schini VB, Sundt TM, Jr., and Vanhoutte PM**. Reduced production of cGMP underlies the loss of endothelium-dependent relaxations in the canine basilar artery after subarachnoid hemorrhage. *Circ Res* 70: 248-256, 1992.

25. **Kontos HA, Wei EP, Navari RM, Levasseur JE, Rosenblum WI, and Patterson JL, Jr.** Responses of cerebral arteries and arterioles to acute hypotension and hypertension. *Am J Physiol* 234: H371-383, 1978.

26. **Lacza Z, Herman P, Gorlach C, Hortobagyi T, Sandor P, Wahl M, and Benyo Z**. NO synthase blockade induces chaotic cerebral vasomotion via activation of thromboxane receptors. *Stroke* 32: 2609-2614, 2001.

27. **Liebeskind DS**. Collateral circulation. *Stroke* 34: 2279-2284, 2003.

28. **Maeda K, Hata R, Bader M, Walther T, and Hossmann KA**. Larger anastomoses in angiotensinogen-knockout mice attenuate early metabolic disturbances after middle cerebral artery occlusion. *J Cereb Blood Flow Metab* 19: 1092-1098, 1999.

29. **Maeda K, Hata R, and Hossmann KA**. Differences in the cerebrovascular anatomy of C57black/6 and SV129 mice. *Neuroreport* 9: 1317-1319, 1998.

30. **Malinski T, Bailey F, Zhang ZG, and Chopp M**. Nitric oxide measured by a porphyrinic microsensor in rat brain after transient middle cerebral artery occlusion. *J Cereb Blood Flow Metab* 13: 355-358, 1993.

31. **Millikan CH**. Cerebral circulation: clinical concepts as effected by vascular anatomy, pathology, and pathophysiology. *Clin Neurosurg* 16: 419-435, 1969.

32. **Moncada S, Palmer RM, and Higgs EA**. Nitric oxide: physiology, pathophysiology, and pharmacology. *Pharmacol Rev* 43: 109-142, 1991.

33. **Morikawa E, Huang Z, and Moskowitz MA**. L-arginine decreases infarct size caused by middle cerebral arterial occlusion in SHR. *Am J Physiol* 263: H1632-1635, 1992.

34. **Morikawa E, Rosenblatt S, and Moskowitz MA**. L-arginine dilates rat pial arterioles by nitric oxide-dependent mechanisms and increases blood flow during focal cerebral ischaemia. *Br J Pharmacol* 107: 905-907, 1992.

35. **Morita Y, Fukuuchi Y, Koto A, Suzuki N, Isozumi K, Gotoh J, Shimizu T, Takao M, and Aoyama M**. Rapid changes in pial arterial diameter and cerebral blood flow caused by ipsilateral carotid artery occlusion in rats. *Keio J Med* 46: 120-127, 1997.

36. **Mozaffarian D, Benjamin EJ, Go AS, Arnett DK, Blaha MJ, Cushman M, Das SR, de Ferranti S, Despres JP, Fullerton HJ, Howard VJ, Huffman MD, Isasi CR, Jimenez MC, Judd SE, Kissela BM, Lichtman JH, Lisabeth LD, Liu S, Mackey RH, Magid DJ, McGuire DK, Mohler ER, 3rd, Moy CS, Muntner P, Mussolino ME, Nasir K, Neumar RW, Nichol G, Palaniappan L, Pandey DK, Reeves MJ, Rodriguez CJ, Rosamond W, Sorlie PD, Stein J, Towfighi A, Turan TN, Virani SS, Woo D, Yeh RW, and Turner MB**. Heart Disease and Stroke Statistics-2016 Update: A Report From the American Heart Association. *Circulation* 133: e38-e360, 2016.

37. **Nishioka H**. Results of the treatment of intracranial aneurysms by occlusion of the carotid artery in the neck. *J Neurosurg* 25: 660-704, 1966.

38. **Okamoto H, Hudetz AG, Roman RJ, Bosnjak ZJ, and Kampine JP**. Neuronal NOS-derived NO plays permissive role in cerebral blood flow response to hypercapnia. *Am J Physiol* 272: H559-566, 1997.

39. **Proweller A, Wright AC, Horng D, Cheng L, Lu MM, Lepore JJ, Pear WS, and Parmacek MS**. Notch signaling in vascular smooth muscle cells is required to pattern the cerebral vasculature. *Proc Natl Acad Sci U S A* 104: 16275-16280, 2007.

40. **Robertson BE, Schubert R, Hescheler J, and Nelson MT**. cGMP-dependent protein kinase activates Ca-activated K channels in cerebral artery smooth muscle cells. *Am J Physiol* 265: C299-303, 1993.

41. **Rosenblum WI, Nishimura H, and Nelson GH**. Endothelium-dependent L-Arg- and L-NMMA-sensitive mechanisms regulate tone of brain microvessels. *Am J Physiol* 259: H1396-1401, 1990.

42. **Schmidt-Kastner R, Hossmann KA, and Ophoff BG**. Pial artery pressure after one hour of global ischemia. *J Cereb Blood Flow Metab* 7: 109-117, 1987.

43. **Scremin OU, Holschneider DP**. Vascular Supply. In: *The Mouse Nervous System*, edited by Watson C, Paxinos G, Puelles L: Academic Press, 2012.

44. **Shapiro HM, Stromberg DD, Lee DR, and Wiederhielm CA**. Dynamic pressures in the pial arterial microcirculation. *Am J Physiol* 221: 279-283, 1971.

45. **Sokoloff L**. The metabolism of the central nervous system *in vivo*. In: *Handbook of Physiology-Neurophysiology*, edited by Field J, Magoun HW, Hall VE: American Physiological Society, 1960.

46. **Stauss HM, Godecke A, Mrowka R, Schrader J, and Persson PB**. Enhanced blood pressure variability in eNOS knockout mice. *Hypertension* 33: 1359-1363, 1999.

47. **Stauss HM, Nafz B, Mrowka R, and Persson PB**. Blood pressure control in eNOS knock-out mice: comparison with other species under NO blockade. *Acta Physiol Scand* 168: 155-160, 2000.

48. **Sugawa M, Koide T, and Takato M**. BY-1949 elicits vasodilation via preferential elevation of cyclic GMP levels within the cerebral artery: possible involvement of endothelium-mediated mechanisms. *Eur J Pharmacol* 215: 57-62, 1992.

49. **Taylor DW**. Beneficial effect of carotid endarterectomy in symptomatic patients with high-grade carotid stenosis. *N Engl J Med* 325: 445-453, 1991.

50. **Toriumi H, Tatarishvili J, Tomita M, Tomita Y, Unekawa M, and Suzuki N**. Dually supplied T-junctions in arteriolo-arteriolar anastomosis in mice: key to local hemodynamic homeostasis in normal and ischemic states? *Stroke* 40: 3378-3383, 2009.

51. **Toth P, Tarantini S, Davila A, Valcarcel-Ares MN, Tucsek Z, Varamini B, Ballabh P, Sonntag WE, Baur JA, Csiszar A, and Ungvari Z**. Purinergic glio-endothelial coupling during neuronal activity: role of P2Y1 receptors and eNOS in functional hyperemia in the mouse somatosensory cortex. *Am J Physiol Heart Circ Physiol* 309: H1837-1845, 2015.

52. **Vander Eecken HM, and Adams RD**. The anatomy and functional significance of the meningeal arterial anastomoses of the human brain. *J Neuropathol Exp Neurol* 12: 132-157, 1953.

53. **Wang Q, Pelligrino DA, Baughman VL, Koenig HM, and Albrecht RF**. The role of neuronal nitric oxide synthase in regulation of cerebral blood flow in normocapnia and hypercapnia in rats. *J Cereb Blood Flow Metab* 15: 774-778, 1995.

54. **Yamaguchi S, Kobayashi S, Murata A, Yamashita K, and Tsunematsu T**. Effect of aging on collateral circulation via pial anastomoses in cats. *Gerontology* 34: 157-164, 1988.

55. **Youmans JR, Kindt GW, and Mitchell OC**. Extended studies of direction of flow and pressure in the internal carotid artery following common carotid artery ligation. *J Neurosurg* 27: 250-254, 1967.

56. **Zhang H, Prabhakar P, Sealock R, and Faber JE**. Wide genetic variation in the native pial collateral circulation is a major determinant of variation in severity of stroke. *J Cereb Blood Flow Metab* 30: 923-934, 2010.

57. **Zhang ZG, Chopp M, Zaloga C, Pollock JS, and Forstermann U**. Cerebral endothelial nitric oxide synthase expression after focal cerebral ischemia in rats. *Stroke* 24: 2016-2021, 1993.

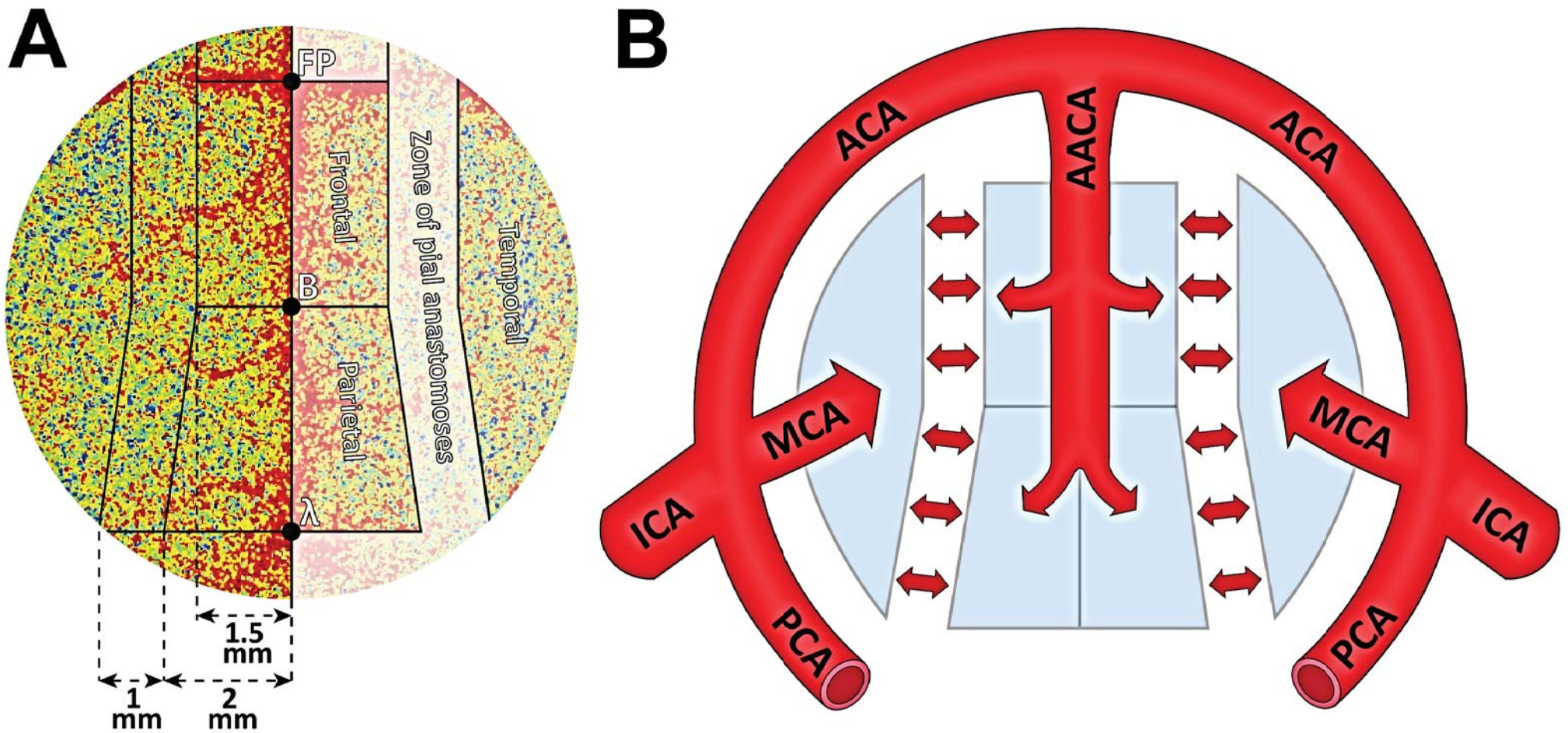
A
FP
Frontal
Zone of pial anastomoses
Temporal
Parietal
λ
1.5 mm
1 mm
2 mm
B
ACA
AACA
ACA
MCA
MCA
ICA
ICA
PCA
PCA

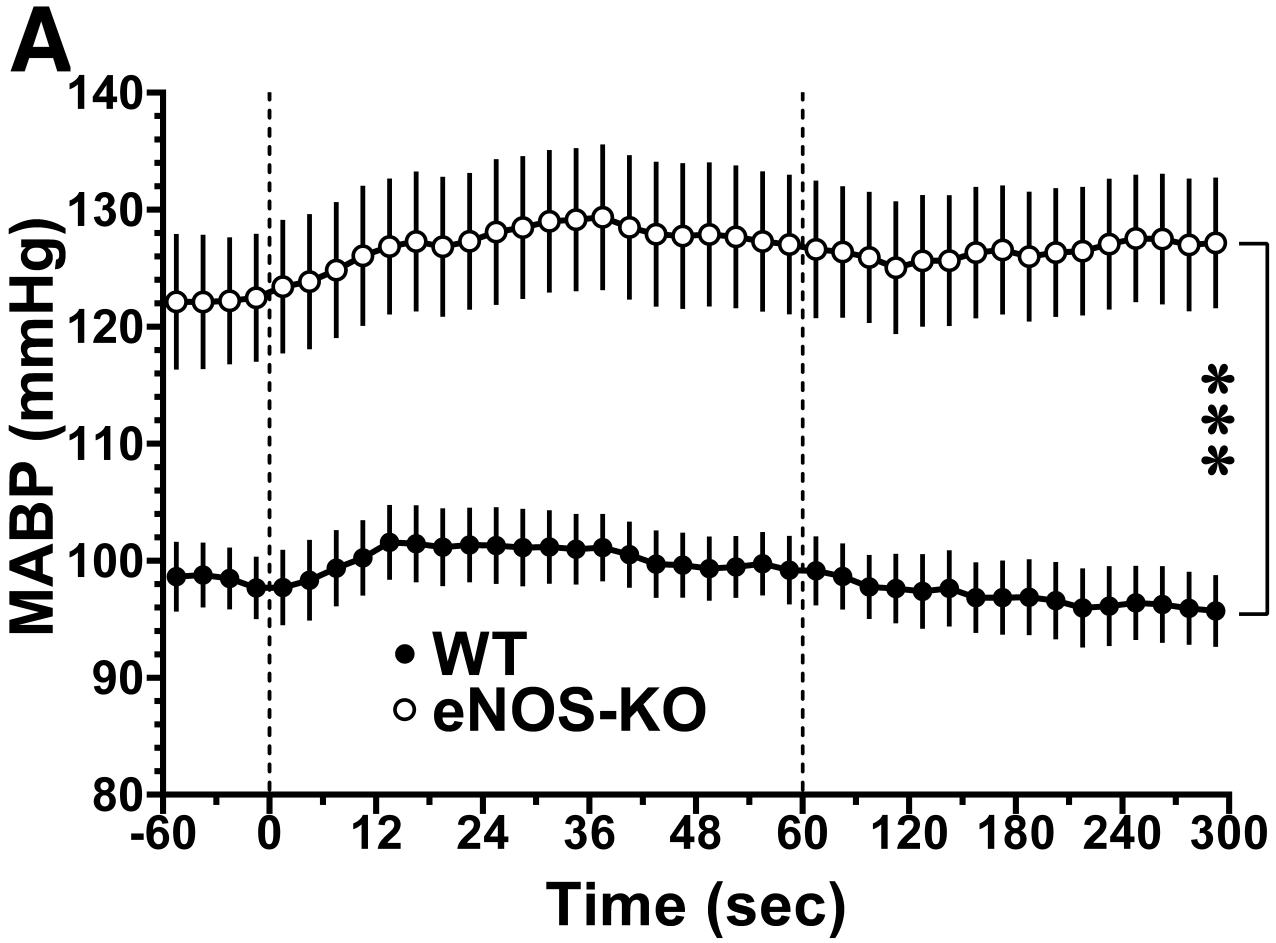
A
MABP (mmHg)
140
130
120
110
100
90
80
***
• WT
○ eNOS-KO
-60
0
12
24
36
48
60
120
180
240
300
Time (sec)

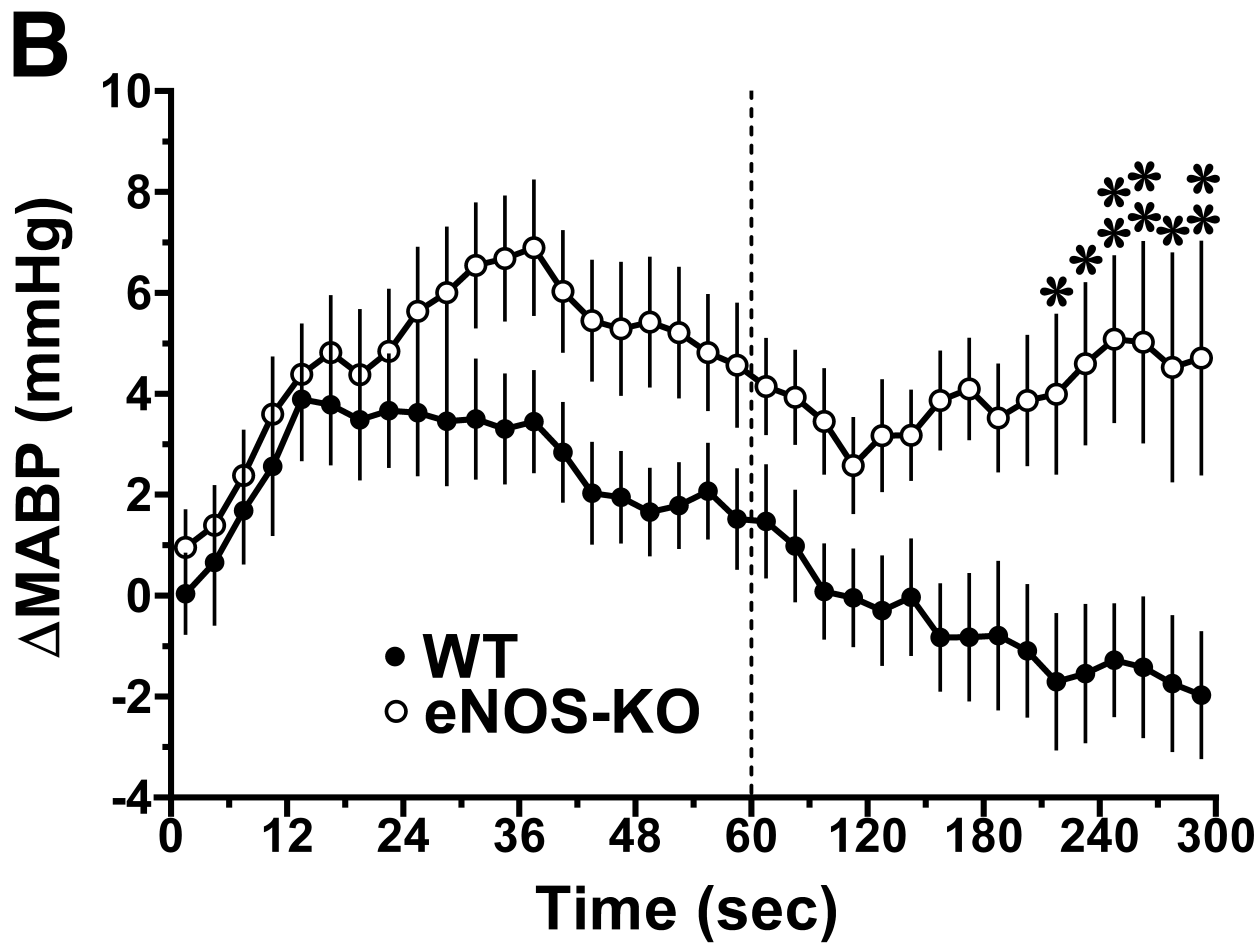
B
ΔMABP (mmHg)
10
8
6
4
2
0
-2
-4
• WT
○ eNOS-KO
0
12
24
36
48
60
120
180
240
300
Time (sec)

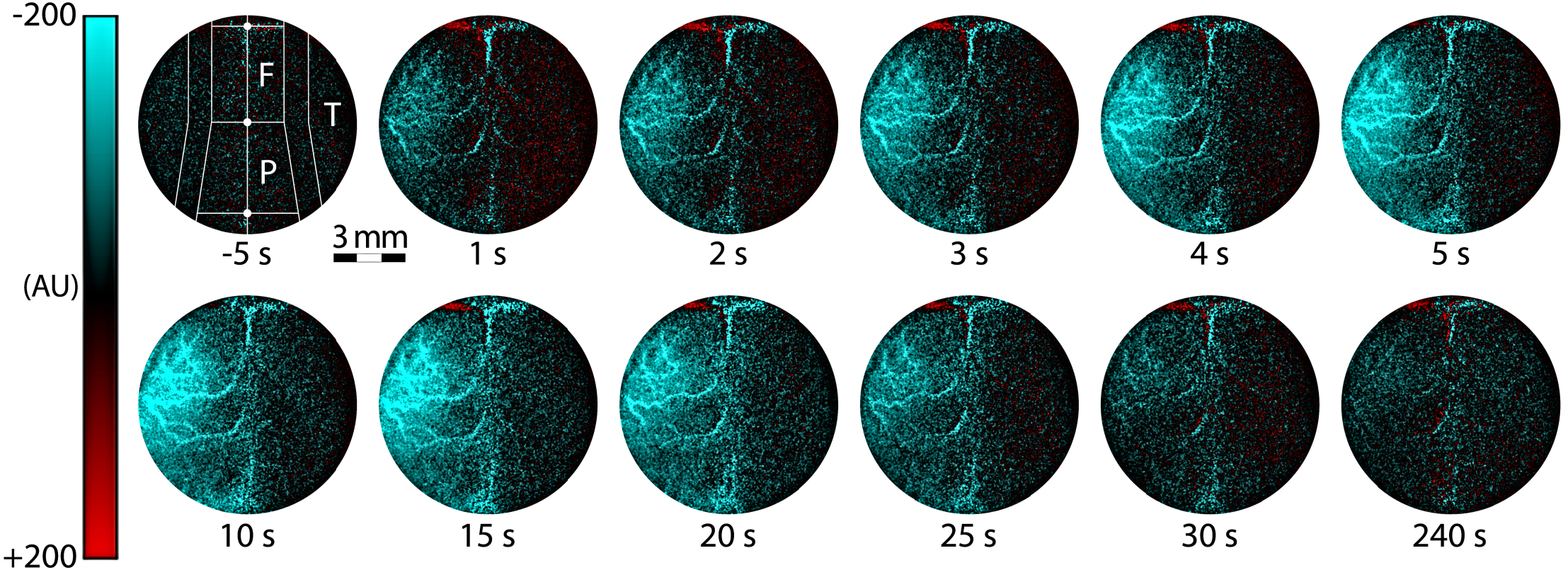
-200
(AU)
+200
F
T
P
3 mm
-5 s
1 s
2 s
3 s
4 s
5 s
10 s
15 s
20 s
25 s
30 s
240 s

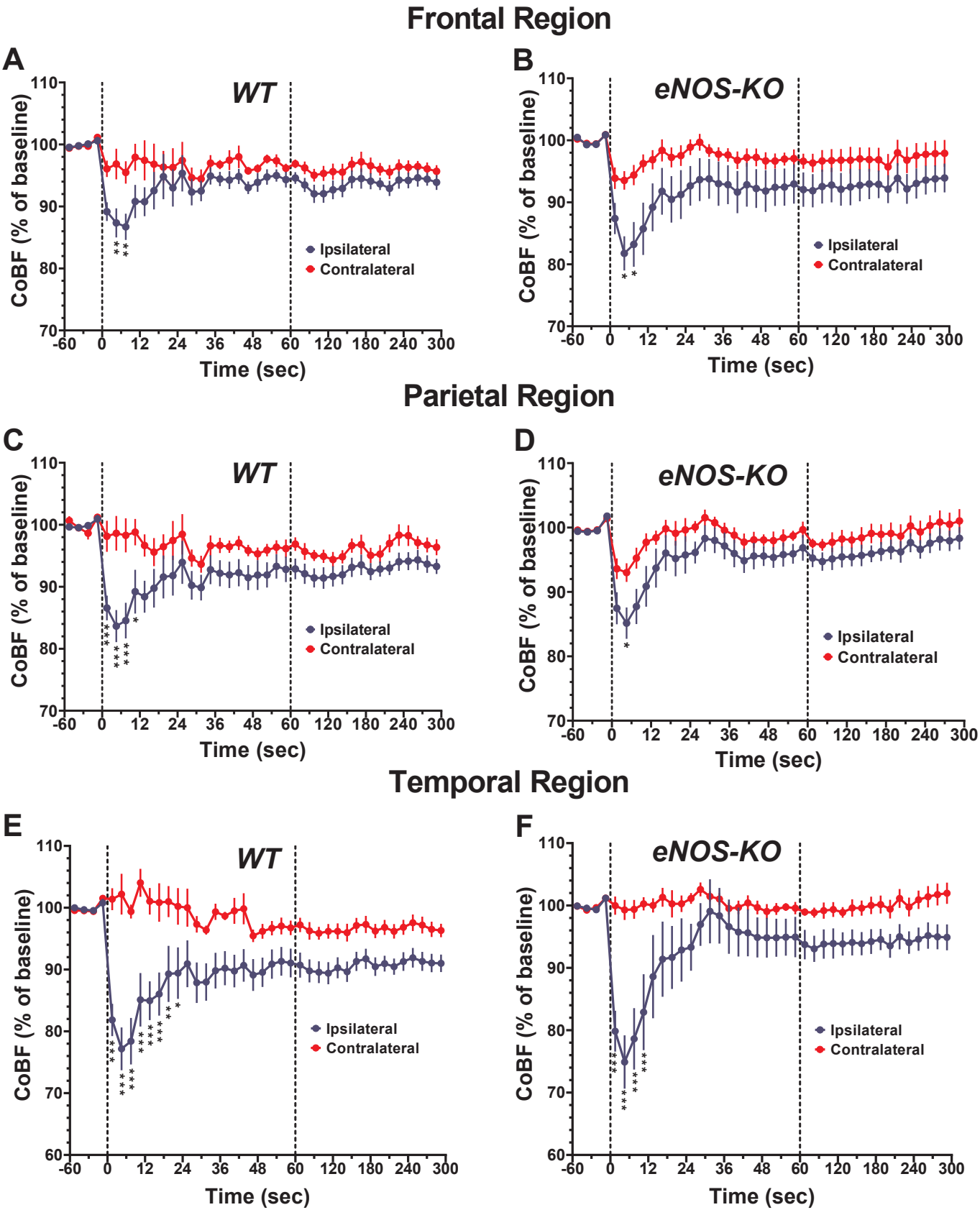
Frontal Region
A
WT
B
eNOS-KO
Parietal Region
C
WT
D
eNOS-KO
Temporal Region
E
WT
F
eNOS-KO
CoBF (% of baseline)
Time (sec)
Ipsilateral
Contralateral

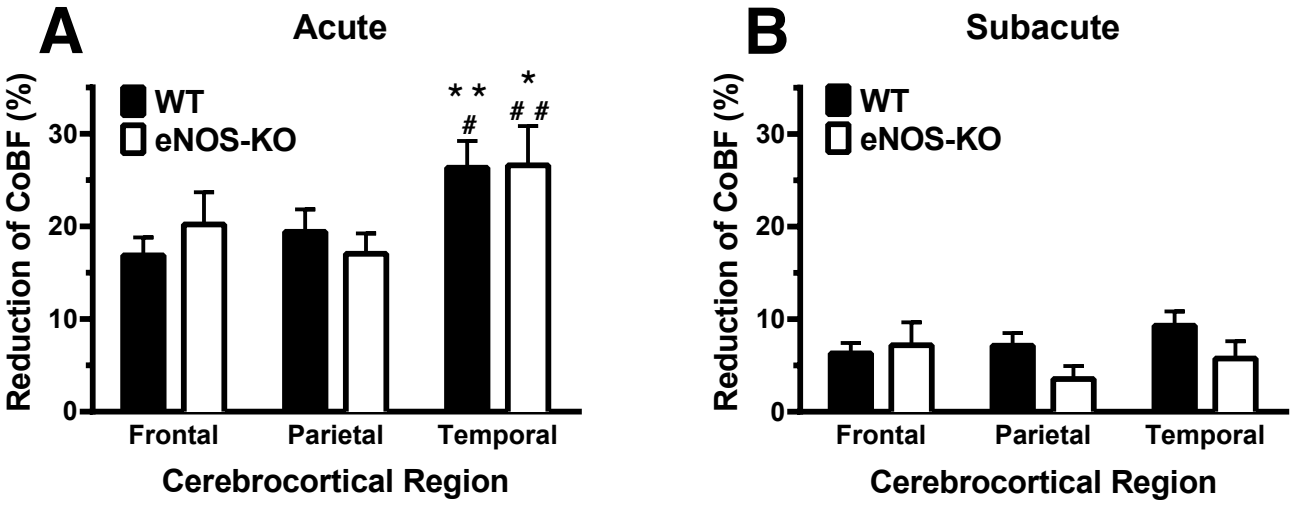
A
Acute
WT
eNOS-KO
Reduction of CoBF (%)
0
10
20
30
* *
#
*
# #
Frontal
Parietal
Temporal
Cerebrocortical Region
B
Subacute
WT
eNOS-KO
Reduction of CoBF (%)
0
10
20
30
Frontal
Parietal
Temporal
Cerebrocortical Region